EEG-Based Semantic Vigilance Level Classification Using Directed Connectivity Patterns and Graph Theory Analysis

FARES AL-SHARGIE[1,2], (Member, IEEE), **OMNIA HASSANIN**[2], (Member, IEEE),
USMAN TARIQ[1,2], (Member, IEEE), **AND HASAN AL-NASHASH**[1,2], (Senior Member, IEEE)
[1]Department of Electrical Engineering, American University of Sharjah, Sharjah, United Arab Emirates
[2]Department of Biomedical Engineering, American University of Sharjah, Sharjah, United Arab Emirates

Corresponding author: Fares Al-Shargie (fyahya@aus.edu)

ABSTRACT This paper proposes two novel methods to classify semantic vigilance levels by utilizing EEG directed connectivity patterns with their corresponding graphical network measures. We estimate the directed connectivity using relative wavelet transform entropy (RWTE) and partial directed coherence (PDC) and the graphical network measures by graph theory analysis (GTA) at four frequency bands. The RWTE and PDC quantify the strength and directionality of information flow between EEG nodes. On the other hand, the GTA of the complex network measures summarizes the topological structure of the network. We then evaluate the proposed methods using machine learning classifiers. We carried out an experiment on nine subjects performing semantic vigilance task (Stroop color word test (SCWT)) for approximately 45 minutes. Behaviorally, all subjects demonstrated vigilance decrement as reflected by the significant increase in response time and reduced accuracy. The strength and directionality of information flow in the connectivity network by RWTE/PDC and the GTA measures significantly decrease with vigilance decrement, $p < 0.05$. The classification results show that the proposed methods outperform other related and competitive methods available in the literature and achieve 100% accuracy in subject-dependent and above 89% in subject-independent level in each of the four frequency bands. The overall results indicate that the proposed methods of directed connectivity patterns and GTA provide a complementary aspect of functional connectivity. Our study suggests directed functional connectivity with GTA as informative features and highlight Support Vector Machine as the suitable classifier for classifying semantic vigilance levels.

INDEX TERMS Vigilance decrement, electroencephalogram, relative wavelet transform entropy, partial directed coherence, graph theory analysis, machine learning.

I. INTRODUCTION

Vigilance refers to the mental capacity to sustain attention over an extended time. Previous research has demonstrated that cognitive performance typically declines with time on task (TOT), which is a phenomenon commonly denoted as the vigilance decrement [1], [2]. Different vigilance tasks can significantly affect the degree of vigilance decrement. In particular, complex vigilance tasks are mentally demanding and stressful [3]. In this context, mental effort and frustration

are the major contributors to the high levels of perceived cognitive workload in vigilance tasks. The cognitive resource theory of vigilance decrement has stated that during the performance of high workload, cognitive resources become depleted, leading to decrement in perceptual sensitivity [4]. The underload theory predicts a faster decrement in less challenging tasks. This decrement has been alternatively ascribed to either withdrawal of the supervisory attentional system, due to under arousal caused by the insufficient workload, or to a decreased attentional capacity and thus the impossibility to sustain mental attention [5]. In particular, vigilance decrement is a severe matter of a broad array of work

The associate editor coordinating the review of this manuscript and approving it for publication was M. Anwar Hossain.

environments, including surveillance, airport security, industrial control, driving and medical monitoring [2], [6]. In all these domains, individuals are required to keep the mental states with high vigilance level. Hence, an effective method of detecting vigilance levels is of paramount importance to prevent vigilance-related risks and productivity losses.

Several physiological indicators, such as electrocardiogram (ECG), electrooculogram (EOG) [7], electromyogram (EMG) [8], eye-closure [9], [10] and electroencephalogram (EEG) [11]–[13] have been used for vigilance level detection. However, identifying reliable and valid biomarkers remains a challenge within the research community. EEG has been regarded as one of the most reliable and effective measurements for identifying vigilance state since it is the direct reaction of the brain states [14]. Besides, EEG technology is safe, non-invasive, low cost, easy to operate, and has high temporal resolution. The transitions of vigilance state are usually accompanied by the changes in the power spectrum in EEG, suggesting a robust and efficient way for vigilance level detection. Spectral powers in typical frequency bands are closely related to vigilance decrement. Data analysis presented in this study involve four frequency bands, [delta (< 4 Hz), theta (4–7 Hz), alpha (8–12 Hz), and beta (13–30 Hz) frequency bands]. Different brain regions may show different level of sensitivities to vigilance levels. Generally speaking, studies have reported frontal increase in alpha and theta power, during vigilance decrement, which indicates a loss of cortical arousal [13], [15]–[17].

Meanwhile, other studies showed that alpha and theta bands activities in the central and occipital regions are more correlated to fatigue due to vigilance tasks [18]–[20]. In line with these findings, Parikh and Micheli-Tzanakou [21] found an increased power of alpha and theta associated with a decreased power of beta at the occipital area of the brain. In particular, the alpha rhythm increased when human's vigilance level decreased, while at the same time, the beta rhythm decreased [22], [23]. Interestingly, alpha rhythm has subsequently proved to be diagnostic of cognitive fatigue and loss of alertness in a range of applied settings [24]–[27]. An increase in frontal sites near 4 Hz theta and decrease near 40 Hz gamma have specifically been correlated with reduced arousal drowsiness [28]. Particularly, frontal theta power typically increased with mental workload and demands on working memory [29], suggesting its sensitivity to mental effort associated with vigilance decrement [30], [31].

Some studies have reported that occipital alpha and beta, in addition to, frontal delta and theta decrease with vigilance decrement [32], [33]. The phenomenon where the alpha peak frequency exhibits a slight decrease is observed during the transition to drowsiness. This is in line with a study that showed beta band significantly decreased during the state of driving sleepiness. The decrease appeared in frontal [19], central [34], and temporal [34] regions. Delta and gamma bands were also reported to be associated with drowsiness [34]. However, it remains unclear which frequency band and brain region is highly sensitive to changes in resource utilization during vigilance decrement due to a complex task. In particular, most of the studies describe the EEG signals of a single channel in a local brain region and do not involve the interactions between brain regions. Ishii *et al.* [35] have demonstrated that the complex neural mechanism of mental fatigue in vigilance tasks included a facilitation system and an inhibition system involving a wide range of brain regions, not limited to task-related regions. In line with that, few studies have utilized functional connectivity to estimate the functional coupling between brain regions under fatigue [36]–[38]. The studies found that when mental fatigue level increases due to vigilance tasks, the functional coupling decreased, specifically over the parietal-to-frontal areas in individual theta, alpha and beta frequency bands. However, for the simulated driving task, studies have reported an increase in the connectivity network in the frontal-central, and central-parietal/occipital areas at the end of driving sessions [39]–[41]. Besides, a recent study has reported both; decrease and increase in the connectivity networks in driving fatigue [42]. The decreased connections were found across most of the brain regions, while the increased connections were found from frontal to parietal or occipital regions. It seems that the frontal region is still an essential part during the alert and fatigue states. Besides, the occipital region is related with the visual task.

To date, few studies have utilized vigilance tasks that involve cognition and sensory processes. In the present work, we aim at studying the neural mechanism of vigilance state while doing novel semantic vigilance task using SCWT. In semantic vigilance tasks, operators are required to respond to targets that are lexical and withhold response to neutral stimuli, which are not semantically representative or related to target signals. Thus, the tasks are unique in that they do not fall neatly into the cognitive sensory vigilance distinction and involve both cognitive and sensory processes. In particular, the semantic task requires high mental demand, high effort and frustration. To this end, we propose to utilize RWTE and PDC to estimate the functional connectivity and GTA to summarize the topological structure of the network for vigilance levels. Data analysis presented in this study involves the four frequency bands, due to the unknown influence of vigilance decrement on frequency bands with respect to a semantic task. Furthermore, we assessed the feasibility of applicable vigilance detection through five different classifiers: K-Nearest Neighbors (KNN), Linear Discriminant Analysis (LDA), Decision Tree (DT), Naïve Bayes Classifier (NBC), and Support Vector Machines (SVM).

This paper is organized as follows. Section II describes the participants, experiment protocol, data acquisition and signal preprocessing. Section III presents the proposed methods of EEG connectivity, graph theory analysis, feature extraction, statistical analysis and classification. Section IV presents the results of connectivity and classification. Section V provides a detailed discussion on the findings. Finally, section VI concludes this paper.

II. EXPERIMENT

A. PARTICIPANTS

Nine healthy young students from the American University of Sharjah (age: 22 ± 2 years, (mean ± standard deviation)) have participated in this study. All participants had normal or corrected to normal vision and no reported hearing deficits/difficulties. Besides, they had no history of neurological or psychiatric illnesses and had no current or prior use of psychoactive medication. The experiment was conducted between 3.00 pm and 7.00 pm to avoid the influences of circadian rhythm on cognitive vigilance performance [43]. The aims and procedures of the experiment were explained to all the subjects before commencing the experiment. They were asked to give a written informed consent before participation in the study. The participants were free to stop their participation during the experiment or to withdraw from the experiment for any reason. All participants were asked to abstain from caffeine, exercise, energy drink, and tobacco use for 24 hours before testing. All methods performed followed the Declaration of Helsinki. The Institutional Review Board of the American University of Sharjah approved the experiment.

B. EXPERIMENT PROOCOL

The experiment task was designed based on SCWT and presented to participants using a graphical user interface designed with MATLAB (Mathworks, Natick, MA). The SCWT involved six color words (such as ['Blue', 'Green', 'Red', 'Magenta', 'Cyan', and 'Yellow']) presented randomly on the computer monitor and the answer for each color word to be matched was presented in random sequences. Only one color-word is displayed on the monitor screen at a time, see FIGURE 1(a). The displayed color-word is written in a different color than the word's meaning. The correct answer for the color-word is the color in which the word is displayed. The participants pick their answers as quickly and accurately as possible by left-clicking the mouse on one of the six answering buttons as shown in FIGURE 1(a). The matching answers were presented with random colored-background to add more attention to the task. Answering incorreclty or failing to answer each question within the allocated time, would present feedback to the participants on their performance, i.e. a message of "Correct" or "Wrong" or "Time is out" is displayed on the monitor.

Behavioral data such as reaction time (RT) to stimuli and accuracy of detection were collected while solving the task. In this task, four indicators measure participants' attention levels: commission error, omission error, reaction time and accuracy. A commission error occurs when a participant fails to inhibit the response and incorrectly responds to a non-color word. In contrast, an omission error occurs when a participant is unable to pick-up or react to the color word. Once participants' responses are checked, the time they spent on task is recorded. The RT is measured as the average time it takes for the participant to respond correctly to a target stimulus.
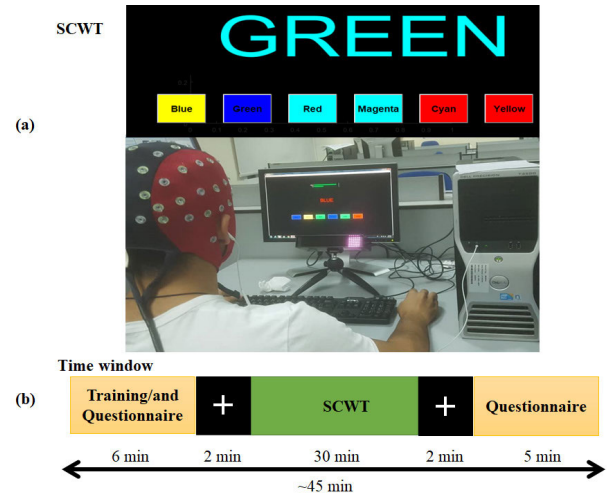

FIGURE 1. The experimental design a) Stroop color-word task (SCWT) presentation interface and b) timing window. In the timing window, the plus sign in black background is for the pre and post-baseline. Thirty (30) min SCWT is for the vigilance task presentation.

The number of trials also depended on the participant's rating speed. Different markers were sent to mark the start and the end of epochs in each SCWT question. The overall accuracy is calculated based on the number of the color word correctly matched over the total number of the displayed color word targets.

The overall experimental time frame for each participant included 6 minutes for training and filling the questionnaire, 2 minutes for pre-baseline, 30 minutes for performing SCWT, 2 minutes for post-baseline and 5 minutes for filling another survey. FIGURE 1(b) shows the time window of the experiment.

The questionnaire used in this study was based on Brunel Mood Scale (BRMUS) [44]. All participants filled-in the questionnaires before and after they performed the semantic vigilance task. The BRMUS composed of 32 items. These items correspond to an 8-factor model including "Anger," "Tension", "Confusion," "Depression," "Fatigue," "Happy," "Calmness" and "Vigor." Each item has 5-point Likert scale ranges from '0' to '4' representing "not at all" to "extremely" depending on the participant's feelings.

C. DATA ACQUISITION AND PREPROCESSING

EEG data was recorded using 64 Ag/AgCl scalp electrodes according to the standard 10–20 system (Waveguard, ANT B.V., Netherlands) at a sampling rate of 500 Hz. Electrode impedance was kept below 10 kΩ throughout all the recordings and referenced to the left and right mastoids; M1 and M2. Main interferences were avoided by anti-aliasing with a band-pass (0.5-70 Hz) and a 50 Hz notch filter.

Raw EEG signals were preprocessed using EEGLAB toolboxes (9.0.4) [45] as well as using custom scripts developed in our previous studies [46]–[49]. The raw EEG signals were band-pass filtered using a finite impulse response (FIR) filter

with 0.1 Hz to 30 Hz bandwidth. All the EEG signals were then re-referenced to the common average reference and segmented into target-related EEG epochs of 1200 ms. Independent Component Analysis (ICA) was then employed to remove noise. We extracted the baseline and removed it using the whole duration of each epoch. The epochs were baseline corrected by subtracting the -100 to 0 milliseconds prestimulus baseline from all data points in the epoch. Finally, all EEG epochs were visually double-checked to eliminate data segments contaminated with noise.

Then, we defined two types of vigilance states for subjects within the 30-min EEG recordings: 1) the alert state/high vigilance, including the first 5 min of EEG signals (corresponding to 80 trials) while doing the SCWT, 2) the vigilance decrement state, which referred to the last 5 min of EEG signals within the SCWT (corresponding to 80 trials). Then we investigated the relative wavelet transform entropy and partial directed coherence in each trial to quantify the strength and directionality of information flow between nodes. Besides, we estimated the complex network measures to summarize the topological structure of the network for each mental state at four different frequency bands.

III. METHODOLOGY

A. RELATIVE WAVELET TRANSFORM ENTROPY

First, we employed wavelet analysis through the Orthogonal Discrete Wavelet Transform (ODWT) to obtain the wavelet coefficients series at 4-different resolutions for each EEG channel, one for each brain rhythm [50]. Data analysis, presented in this study, involves four frequency bands; [δ wavelet (0.1 $\sim$4Hz), θ wavelet (4$\sim$8Hz), α wavelet (8$\sim$13Hz), and β wavelet (14$\sim$30Hz)], as described in [51], [52]. The ODWT for a given EEG signal $X(t)$ is obtained using:

$$X(t) = \sum_{j=1}^{4} \sum_{k=1}^{600} d_j(k)\psi_{j,k}(t), \qquad (1)$$

where, $d_j(k)$ is the wavelet coefficient at time interval k (k=1200ms or 600 EEG data points). Then, the subband wavelet entropy is defined in terms of the relative wavelet energy of the wavelet coefficients. The energy at each resolution level $j = 1 \ldots 4$, is estimated by squaring and summing the wavelet coefficients $d(k)$ corresponding to each EEG rhythm:

$$E_j = \sum_{k} \left| d_j(k) \right|^2, \quad j = 1 \ldots 4 \qquad (2)$$

The total energy of the wavelet coefficients are then calculated using:

$$E_{total} = \sum_{j=1}^{4} E_j \qquad (3)$$

The relative energies at each level are estimated by dividing each absolute energy value with the total energy:

$$p_j = E_j / E_{total} \qquad (4)$$

Obviously, $\sum_j p_j = 1$ and the distribution is considered as time-scale density. The wavelet entropy for each trial is, in turn defined as:

$$WE_m = -\sum_j m(p_j) \log_2 m(p_j),$$
$$j = 1, 2, \ldots .4, \ m = 1, 2, \ldots N \qquad (5)$$

where $m(p_j)$ is the relative wavelet energy of channel m and N is the number of nodes.

Second, to obtain the relative wavelet transform entropy RWTE we regard each channel as a node and then determine the connections between nodes m and n in term of the relative wavelet entropy calculated using the following equation:

$$RWTE(m|n) = \sum_j m(p_j) \log_2 \left[\frac{m(p_j)}{n(p_j)} \right],$$
$$j = 1, 2, \ldots 4, \quad m = 1, 2, \ldots N, \ n = 1, 2, \ldots, N \qquad (6)$$

where $m(p_j)$ and $n(p_j)$ represent the relative wavelet energy of channel m and n, respectively, and N is the number of nodes. The directed RWTE values are stored in N×N matrix, which is not symmetric with reference to the main diagonal.

B. PARTIAL DIRECTED COHERENCE

PDC is a multivariate spectral measure used to determine the directed influences of Granger causality between EEG signals in a multivariate set.

Let $X(n) = [x_1(n), x_2(n), \ldots, x_N(n)]^T$ represents an N channel EEG signal (N=62 in this study), then a multivariate model with m channels of EEG signals and order p is defined by Eq. 7:

$$X(n) = \sum_{r=1}^{p} A_r X(n-r) + W(n), \qquad (7)$$

where $W(n)$ is a white Gaussian noise with mean zero, and the matrix A_r contains the coefficient matrix, p is the order of multivariate autoregressive model (MVAR) determined using Akaike information criterion (AIC) [53] according to:

$$AIC(p) = 2 \log[\det(\Sigma)] + \frac{2N^2 p}{N_{total}}, \qquad (8)$$

where, $\det(\Sigma)$ denotes the covariance matrix of noise vector $W(n)$ and N_{total} is the total number of EEG samples in all trials. In the present study, the average MVAR model order p for all subjects was 7. Once the coefficients of the MVAR model are adequately estimated, a representation of Granger causality in the frequency domain can be obtained from the difference between the N-dimensional identity matrix I and the Fourier transform of the coefficient series Ar ($r = 1, 2, \ldots, p$) according to:

$$A(f) = I - \sum_{r=1}^{p} A_r e^{-j2\pi fr} \qquad (9)$$

Finally, the directional flow of information at frequency f from channel j to channel i is defined as

$$PDC_{i,j}(f) = \frac{|A_{i,j}(f)|}{\sqrt{\sum_k A_{kj}^*(f)A_{kj}(f)}}, \qquad (10)$$

where the asterisk denotes matrix transposition and complex conjugate, A_{ij} are elements of the matrix $A(f)$, and $PDC_{i,j}$ indicates the direction and weight of the information flow from channel j to i at the frequency f. In this study we used a moving time window of 1200ms to compute PDC values. This results in 160 PDC network matrices (each has the size of 62×62 weighted directed matrix) that are created for each subject in each frequency band. PDC gives values in the range between [0, 1]. High value indicates higher interaction between the two nodes.

The statistical significance of PDC values was then estimated using surrogate analysis. Specifically, the original time series from each channel and epoch were randomly shuffled to remove the phase interactions between signals and then we re-calculated the PDC spectra. An empirical distribution of PDC values under the null hypothesis of no causal relationships was obtained by repeating the surrogate approach 100 times. Based on this observed distribution, the PDC values were considered to be a real connection when they were above the threshold ($p = 0.05$).

C. GRAPH THEORY ANALYSIS (GTA)

Graph theoretical analysis provides quantitative measurements for assessing the topological architecture of a network. We considered six network measures to characterize mental state under alert and vigilance decrement. We use the local: nodal degree (ND), clustering coefficient (CC), local efficiency (LE), and the global: efficiency (GE) transitivity (Tr), and modularity (Q) to characterize the derived complex network. The measures are defined as follows:

NODAL DEGREE (ND): This is the number of edges linked directly to a particular node, which can be regarded as the measure of centrality. For a brain network, degree centrality reflects the cerebral cortex regions that play an essential role in the information transmission and processing of the brain.

CLUSTERING COEFFICIENT (CC): is a measure of network segregation that estimates the degree to which neighboring nodes form complete networks or cliques. For node i, the local clustering coefficient CC is calculated as the ratio between the sum of geometric means of all existing weighted triangles and the number of all possible triangles. In particular, CC measures how well the cluster of node communicates and a high value of CC relates to the high local efficiency of information transfer.

LOCAL EFFICIENCY (LE): is a measure of the fault tolerance of a network (measure of segregation). It verifies whether the communication between nodes is still efficient when a node is removed from the network. Higher LE, indicate the robustness of the network at the local scale.

GLOBAL EFFICIENCY (GE): is a global measure of how efficiently a network exchanges information internally. GE is the average of the inverse of the shortest path between two nodes in the network. GE represents the efficiency of the communication between all the nodes within the network. A network with high global efficiency indicates that, on average, nodes are reached by short communications. The efficiency is then used to quantify the global communication of a network, often referred to "global integration".

TRANSITIVITY (TR): is a simple measure of segregation based on the number of triangles in a network. Tr is a classical version of the clustering coefficient, having the advantages of not influenced by nodes with a low degree.

MODULARITY (Q): The modularity shows the tendency of a network to be partitioned into modules or communities of high internal connectivity and low external connectivity. The modularity is equal to the fraction of sum of the weights of edges that connect nodes in the same community minus what that fraction would be on average if communities remained fixed but the edge weights were randomly distributed [54]. The higher the Q, the more confident one can be that a significant community scatter has been found. The full mathematical expressions of the GTA measures can be found in previous studies [54]–[56].

Because graph-theoretic metrics can be threshold dependent, we examine graph measurements over a range of possible connection strength. Following prior studies [56], results were obtained for common graph sparsity thresholded at the top 30% of individual subject connections.

D. FEATURE EXTRACTION

First, for each subject the RWTE/PDC were computed individually for four frequency bands, each resulting in a total of $4 \times 62 \times 62$ vectorized weighted directed connectivity features per trial (we have a total of 80 trials). Second, a set of complex network matrices (62 clustering coefficients, 62 local efficiency, 1 global efficiency, and 62 node degrees, 1 transitivity and 1 modularity, were derived from the RWTE/PDC matrices for each frequency band as a function of threshold.

E. STATISTICAL ANALYSIS AND CLASSIFICATION

A paired t-test was used to examine (the alert state vs vigilance decrement) differences of subjective, behavioral responses, directed connectivity and graph theory measures of the RWTE and PDC for all the frequency bands. Before conducting the t-test, we used the Kolmogorov-Smirnov test to check if the data is normally distributed [57]. In this paper, we investigated functional connectivity based on strength/weight, directionality and graph theory analysis measures of two different methods discussed above within the four frequency bands. FIGURE 2 shows the flow chart of the proposed method.

To distinguish the two mental states (alert vs. vigilance decrement), we employed five classifiers namely, KNN, LDA, NBC, DT, and SVM. The mathematical formulations of the employed classifiers can be found in [58]–[60].
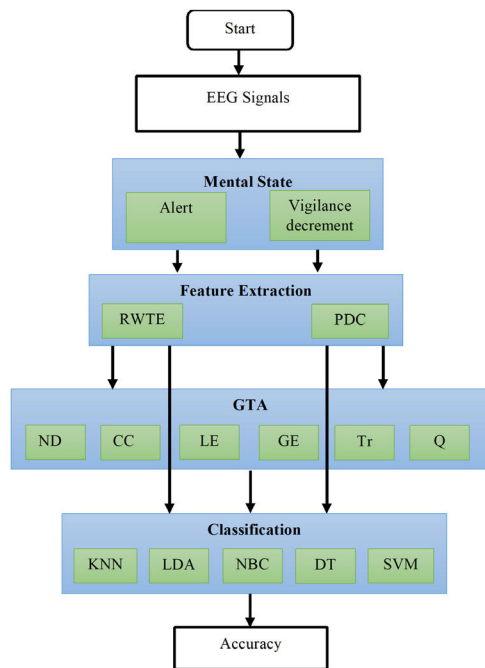
FIGURE 2. Flow chart of the proposed method.

The classifiers were selected due to the fact they are fast and successful classifiers in the field of brain-computer interface (BCI). In addition, we aim to investigate which of the five classifiers perform better in classifying vigilance levels. This will help scientists and researchers to select the most suitable classifier in developing a framework for their vigilance studies. The classifiers are briefly explained below.

K-NEAREST NEIGHBOUR (KNN) is a technique based on minimum distance classifier, that is, the N-labeled sample points in the initial category are selected as the initial center point, distance is calculated from the newly added sample to each category, the nearest category is taken as the category of the sample to be stored, and finally center of each category is updated. In this study, K-value was searched in the interval between 1 and 10 with a step size of 1. The optimal value was then set to 3.

LINEAR DISCRIMINANT ANALYSIS (LDA) is a classifier used to describe the distinctive nature of two or more classes by finding a linear combination of features. These combinations used for dimensionality reduction as a linear classifier for classification. The ratio of between-classes variance to the within-class variance is maximized.

NAIVE BAYES CLASSIFIER (NBC) is a probabilistic classifier based on Bayes theorem. It assumes that the predictor variables are independent random variables. This assumption helps it to compute probabilities required by the Bayes formula from even a small training data. Also if these attributes are not independent, it is possible to obtain a reasonable classification performance.

DECISION TREE (DT) is a classifier used to construct a decision tree with branches and nodes using the extracted feature set. A set of rules representing the different classes is then derived from the tree. These rules are used to predict the class of a new sample with an unknown class.

SUPPORT VECTOR MACHINE (SVM) is a binary classification model constructed in the feature space to find a hyperplane to maximizes the margin between the input data classes. The kernel function of SVM in this study is the Radial Basis Function (RBF), and the learning method is minimal sequential optimization. For fine parameter tuning, we varied the soft margin regularization parameter C from the interval 10^{-2} to 10^{2} with the step of 10 based on cross-validation approach. The most suitable σ in the RBF kernel was searched in the range between 0.5 to 4 (step size of 0.5), and optimal values were set to C = 1 and σ = 3. In all the classifiers, we investigated the classification accuracy of mental state in the form of subject-dependent and subject-independent classification.

SUBJECT-DEPENDENT CLASSIFICATION: we employ 10-fold cross-validation to estimate the classification accuracy. To be concrete, feature sets from the alert state and vigilance-decrement state are randomly and evenly split into 10 equally-sized subsets. We then do training on nine subsets and testing on the remaining one subset. With the aim of obtaining all predicted labels of all samples, we repeat this procedure 10 times so that each subset is used for validation. Thus, the classification accuracy can be defined as the ratio of correctly predicted samples to all samples in the data set. To reduce the deviation of a random partition of the data set in the cross-validation, we perform the 10-fold cross-validation 10 times independently and estimate the final classification accuracy of alert and vigilance-decrement states utilizing the average value of 10 independent implementations of 10-fold cross-validation

SUBJECT-INDEPENDENT CLASSIFICATION: We adopt the leave-one-subject-out (LOSO) cross-validation strategy to evaluate the EEG vigilance level classification performance of the proposed methods. The EEG data of 8-subjects are used for training the classifiers, and the remaining EEG data of one subject is used as testing data. The classifications procedures are repeated such that the EEG data of each subject is used as the testing data. The average classification accuracies and standard deviations corresponding to the propose methods of EEG analysis at the four frequency bands are respectively calculated.

IV. RESULTS

A. BEHAVIORAL DATA

We examined the subjective assessment of vigilance level with the BRMUS scores and found significant effect of task (pre- vs. post experiment) in engagement. Two sample t-test comparing emotional states before and after the SCWT revealed significant reduction of engagement. The statistical analysis showed that anger, tension, vigor, fatigue, and confusion, have significantly increased after performing the task with $p<0.01$, while happy, and calmness have significantly
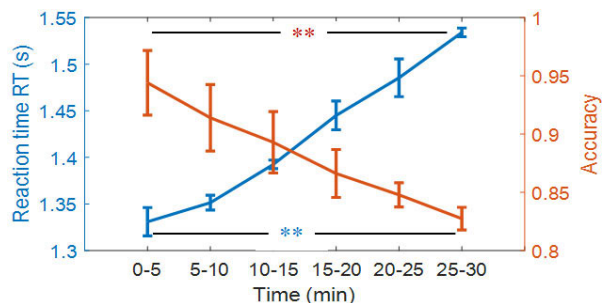
FIGURE 3. Reaction Time and Accuracy in 5-min interval for SCWT. Error bars represent standard deviation of the mean across subjects. The asterisk '**' indicates the differences is significant with p<0.01.

decreased, p<0.05. Then, we investigated the behavioral data (reaction time RT and accuracy) for trial-design SCWT sessions (first 5-min vs. last 5-min). The RT was calculated as the average time taken to answer each question in the SCWT to the number of trials. As expected, we found significant increase in the RT associated with a decrease in the accuracy with *p<0.01*. FIGURE 3 shows the trend of RT and accuracy for the entire 30 min record in 5 min bins for all the subjects. Thus, the overall behavioral results indicate that the 30 min of SCWT was effective in eliciting vigilance decrement to all participants.

B. RWTE AND PDC CONNECTIVITY

The results of connectivity network showed decrement from alertness to vigilance decrement states in most of the EEG nodes. The average differences that are statistically significant in the connectivity strengths and directionalities between the two mental states; alert state - vigilance decrement state (p<0.05), measured by RWTE and PDC, are shown in FIGURE 4 and FIGURE 5, respectively. FIGURE 4 shows the average difference in connectivity strength and directionality measure by RWTE in all the frequency bands (delta $[\delta 1 - \delta 2]$; theta $[\theta 1 - \theta 2]$; alpha $[\alpha 1 - \alpha 2]$; and beta $[\beta 1 - \beta 2]$). Note that the variables $\delta 1$, $\theta 1$, $\alpha 1$ and $\beta 1$ are all for alert state while $\delta 2$, $\theta 2$, $\alpha 2$ and $\beta 2$ are for vigilance decrement state. We only considered the node-strength that is significant at *p<0.05*. The zero value of RWTE shown in the center of the color bar means that the connectivity strength in alert state is equal to the connectivity strength in the vigilance decrement state. Meanwhile, positive value of RWTE indicates significant decrease in the connectivity strength from mental alert to vigilance decrement state and the negative RWTE value indicates significant increment in the connectivity at the vigilance decrement level. By looking at the connectivity network in each frequency band alone as shown in FIGURE 4, it's clearly seen that the differences in the connectivity strength increases from delta to theta to alpha to beta. Specifically, the higher significant differences in the connectivity network (in red color map) are located and directed towards the right hemisphere. Only few electrodes show significant increase in the connectivity strength from
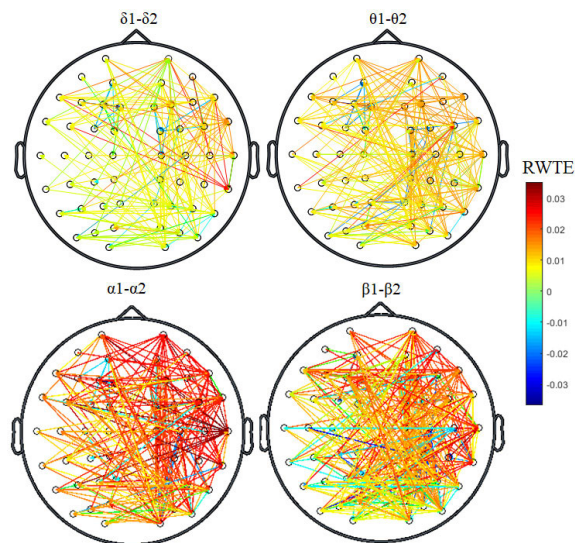

FIGURE 4. Difference in EEG connectivity. Group mean RWTE strength and directionality differences between alert and vigilance decrement in the four frequency bands. The group differences are significantly different at level $\alpha = 0.05$ using two-sample t-test.

FIGURE 5. Difference in EEG connectivity. Group mean PDC strength and directionality differences between alert and vigilance decrement in the four frequency bands. The group differences are significantly different at level $\alpha = 0.05$ using two-sample t-test.
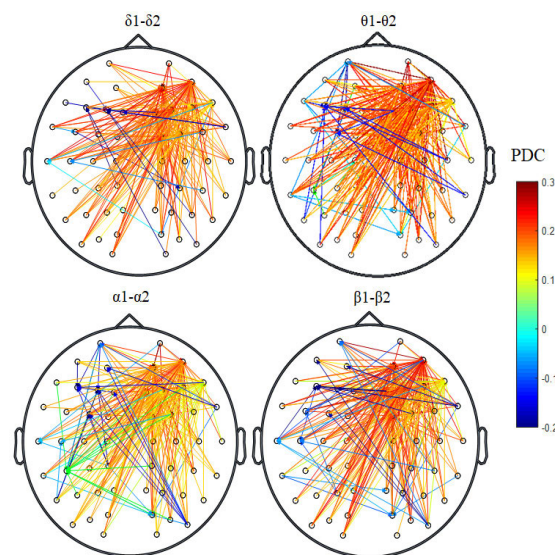
alertness to vigilance decrement at *p<0.05*. The directions of their networks are towards the left hemisphere as shown by the green-to-blue color map in FIGURE 4.

Likewise, connectivity patterns are obtained using PDC. We conducted a statistical analysis on the obtained connectivity network between alertness and vigilance decrement to test if they are significantly different at *p<0.05*. Only the significant connectivity strengths were reconstructed to form the connectivity network. FIGURE 5 shows the differences in connectivity strength and directionality of information flow between alert and vigilance decrement state in all the
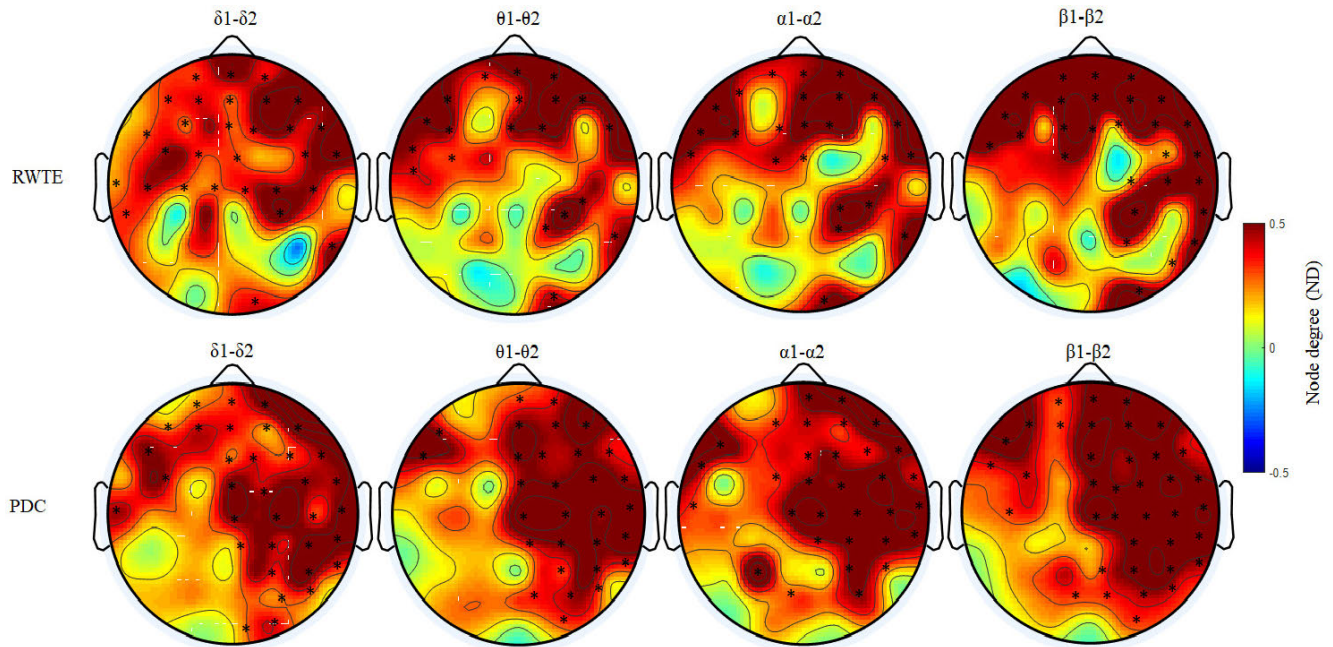
FIGURE 6. Comparison of estimated weighted node degree (in and out degree) averaged over all subjects under the two mental states (alert - vigilance decrement) in the four frequency bands. The asterisk '*' showed the significant electrodes at p < 0.05.

frequency bands (delta [$\delta1 - \delta2$]; theta [$\theta1 - \theta2$]; alpha [$\alpha1 - \alpha2$]; and beta [$\beta1 - \beta2$]). Positive PDC value indicates decrease in the connectivity strength from alertness to vigilance decrement state and negative PDC value indicates increment in the connectivity strength from alertness to vigilance decrement. Interestingly, the connectivity results show that the connectivity network in the right hemisphere are much sensitive to vigilance decrement in all the frequency bands. Meanwhile, small increment in the connectivity network from alertness to vigilance decrement is shown in the left hemisphere in all the frequency bands. It is also noted that the strength of the connectivity network in PDC is much higher than that in RWTE. This shows the superiority of PDC to RWTE. Additionally, from FIGURE 4 and FIGURE 5, it is clearly seen that large quantities of edges are directed towards right hemisphere and frontal brain regions in all the frequency bands.

FIGURE 6 shows the average differences that are statistically significant in the node degree between alert and vigilance decrement states measured by RWTE and PDC in the four frequency bands (delta [$\delta1 - \delta2$]; theta [$\theta1 - \theta2$]; alpha [$\alpha1 - \alpha2$]; and beta [$\beta1 - \beta2$]). The results of the nodal degree in FIGURE 6 show significant decrements *(p<0.05)* from alert to vigilance decrement state in all the bands specifically over the frontal and right hemisphere regions as shown in the topographical maps. Positive ND indicates decrease in the connectivity from alertness to vigilance decrement state and negative ND indicates increment in the connectivity degree. The higher nodal degrees over frontal and right hemisphere in FIGURE 6 (in both; RWTE and PDC) are consistent with the flows of information shown in FIGURE 4 and FIGURE 5.

This support the sensitivity of right hemisphere to vigilance decrement state.

C. GRAPH THEORY ANALYSIS MEASURES

The local graphical analysis of the RWTE and PDC networks shows significant decrement from alert to vigilance decrement states in most of the brain regions as shown in FIGURE 7. FIGURE 7 shows a heat maps of the average differences in clustering coefficient (CC) and local efficiency (LE) between alert and vigilance decrement states in the four frequency bands (delta [$\delta1 - \delta2$]; theta [$\theta1 - \theta2$]; alpha [$\alpha1 - \alpha2$]; and beta [$\beta1 - \beta2$]). Positive value of CC and LE in the heat map indicate decrement in the segregation of the network from alert to vigilance decrement and negative value indicate increment in the segregation. The statistical significant between the two mental state in all the four frequencies is shown by asterisk '$*$' in which single asterisk corresponding to *p<0.05*. Significant node indicates the robustness of the network at the local scale. Notably, the local graphical analysis of CC and LE in PDC shows more significant nodes than that in the RWTE.

Likewise, FIGURE 8 shows the global graphical network analysis under alert (green color) and vigilance decrement (violet color) in the four frequency bands (delta [$\delta1 - \delta2$]; theta [$\theta1 - \theta2$]; alpha [$\alpha1 - \alpha2$]; and beta [$\beta1 - \beta2$]). The distribution of the global network analysis measurements shows significant decrement from alertness to vigilance decrement state in the global efficiency (GE) and Transitivity (Tr) across all subjects at all the frequency bands. Meanwhile, the modularity (Q) measure shows significant increase from
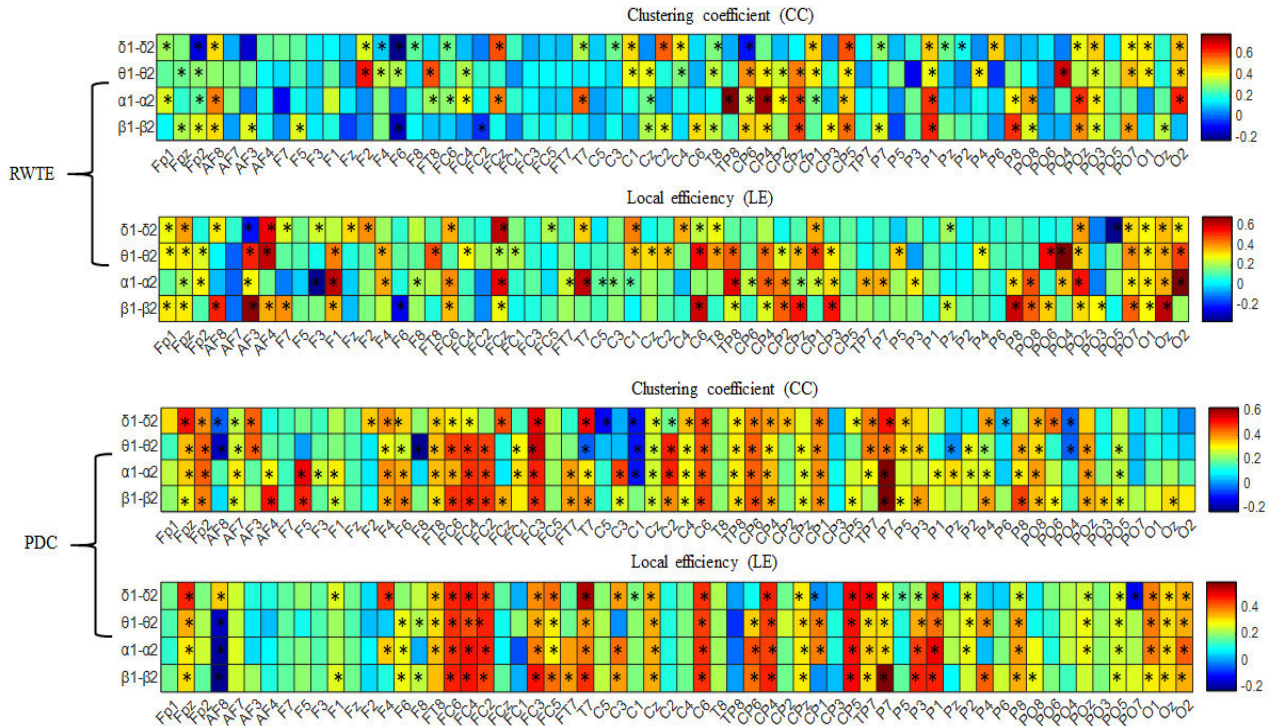
FIGURE 7. Local GTA metrics for the differences between two mental states (alert -vigilance decrement) in the four frequency bands. The strikes. '*', indicate that the differences between the two mental state is significant with p<0.05.
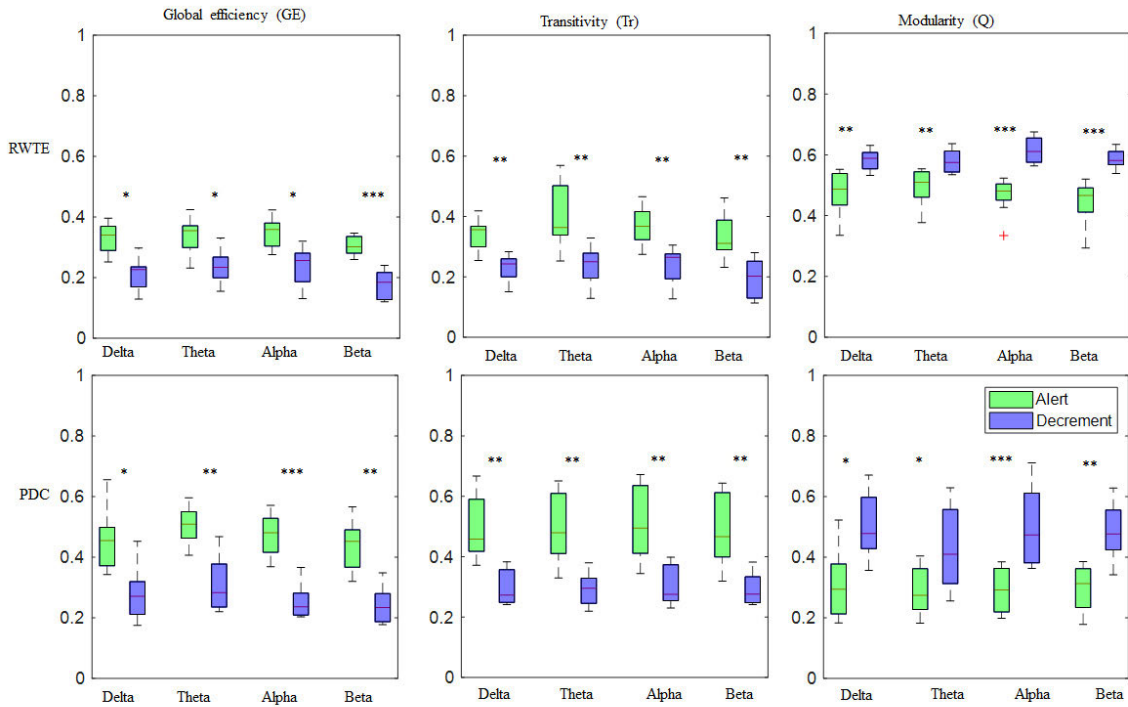
FIGURE 8. Global GTA metrics for two mental states (alert -vigilance decrement) in the four frequency bands. The strikes '*', '**' and '***' indicate that the differences between the two mental state is significant with p<0.05; p<0.01 and, p<0.005, respectively.

alertness to vigilance decrement state. The overall statistical analysis between the alertness and vigilance decrement state as measure by global graphical analysis measurements is

represented by asterisk '$*$' in which single asterisk corresponding to $p<0.05$, and '$**$' correspond to $p<0.01$ and '$***$' equivalent to $p<0.005$. Fascinatingly, higher frequency

at alpha and beta bands show higher significant decrement compared to lower frequency bands indicating their sensitivity to vigilance decrement.

D. CLASSIFICATION

To classify the vigilance levels, we combine the strength and directionality of RWTE/PDC with their corresponding complex network graphical measures to form feature vectors for classification. In particular, we first classified RWTE/PDC separately and found that it can realize the classification with acceptable accuracy. We then combined strength and directionality values of RWTE/PDC with GTA measures (node degree, clustering coefficient, local efficiency, global efficiency, transitivity and modularity) to improve the classification accuracy.

The overall classification results in term of the average accuracies and standard deviations of the proposed methods with the types of classifiers and bands are presented in Table 1 for subject-dependent and in Table 2 for subject-independent classification experiments. The results suggest that RWTE+GTA and PDC+GTA are capable of obtaining intrinsic and effective features from EEG data and the classification accuracy significantly increase using the propose methods. The combination of RWTE/PDC strength and directionality with the GTA measures opens up a new venue to address the challenges in EEG analysis.

Besides, we compared the results of the propose methods with some existing works in EEG classification, including power spectral density feature (PSD) [61], differential entropy (DE), [62] and wavelet entropy (WE) [63]. The PSD, DE and WE features are respectively extracted in each of the frequency bands (δ band, θ band, α band, and β band) to constitute the feature vectors. Feature vectors composed of PSD, DE, and WE were then fed separately into the classifiers to recognize vigilance states. The average classification results of all the methods are also presented in Tables 1 and 2.

From Table 1 and 2, we obtain the following significant points:

- The best classification accuracy is obtained when combining the PDC+GTA in all frequency bands compare to all other methods. With PDC+GTA for subject dependent classification, we achieved 100% accuracy using KNN, LDA, and SVM and 99.2% accuracy using NB and DT. However, for subject independent classification, we achieved 89%, 90%, 92%, 88% and 87% accuracy using KNN, LDA, SVM, NB and DT respectively. For RWTE+GTA in subject dependent analysis, we achieved 98%, 98.2%, 100%, 92%, and 98% accuracy using KNN, LDA, SVM, NB, and DT respectively. Meanwhile, in subject independent experiments we achieved 86% accuracy using KNN, LDA, 98% using SVM, 82% using NB and 87% using DT respectively.
- For most kind of method, the classification accuracies associated with higher frequency bands are better than the ones in the lower frequency bands. Beta band

outperforms other bands with more than 5% in PSD, 3% in DE and 2% in WE in the subject dependent and subject independent under all kind of classifiers. Other methods show higher accuracy in the higher bands compare to lower frequency bands but not significant.

- For each kind of classifier, SVM performs better than other classifiers in all the analysis methods. Thus, we limited our discussion to the results obtained by SVM classifier.

We also conducted one-tailed paired t-test with significance levels 0.05 on the results of every two methods (one proposed vs one baseline method) to validate whether the difference between the means of the two methods is statistically significant. There was a significant improvement in the classification accuracy by the proposed methods compare to the traditional methods as well as to the sole RWTE/PDC methods, p<0.05. We thus, suggest using strength and directionality of RWTE/PDC with their corresponding GTA measures for future vigilance studies.

V. SUMMARY AND DISCUSSION

In this study, we proposed to utilize EEG directed connectivity measured by RWTE and PDC with their corresponding GTA measures to classify semantic vigilance level. To the best of our knowledge, this is the first study to use RWTE+GTA and PDC+GTA to classify semantic vigilance levels. The significant findings are summarized as follows: first, the developed computerized SCWT was effective in eliciting vigilance decrement with time-on-task of 30 minutes as shown in behavioral performance depicted by the reaction time and accuracy in FIGURE 3. Second, a common reduction in the functional connectivity networks (strength and directionality) were revealed in all the frequency bands and methods (RWTE and PDC) under vigilance decrement as shown in FIGURE 4 and FIGURE 5. Third, the local and global graphical analysis of connectivity network demonstrated significant reduction with vigilance decrement in all the frequency bands and methods as shown in FIGURE 6 to FIGURE 8. Fourth, using RWTE/PDC in combination with their corresponding graph theory analysis measures (RWTE+GTA/PDC+GTA) as features, we achieved the highest classification accuracy, in both subject-dependent and subject-independent tests, as summarized in Table 1, and Table 2 respectively. The overall findings are discussed in details in the following paragraphs.

In this study, we found that performing SCWT continuously for 30 minutes significantly influenced the transient state of mood of all participants. It was shown that all participants reported high level of fatigue and confusion after performing the SCWT due to the high cognitive load required to sustain attention to the task. There was a significant decline in behavioral responses from alertness to vigilance decrement state. The average reaction time taken to answer the SCWT increased from the first 5-min to the last 5-min of the task by +14%. Meanwhile, the accuracy of detecting the SCWT

TABLE 1. Comparisons of the average accuracies and standard deviations (%) of subject dependent eeg-based semantic vigilance level classification among the various methods.

Method	Classifier	Delta	Theta	Alpha	Beta
PSD	KNN	82.87±04.85	78.29±16.32	78.41±14.79	93.54±03.00
	LDA	88.07±10.29	83.49±11.80	85.31±10.78	95.09±01.20
	NB	80.39±09.54	75.06±15.65	75.51±15.11	91.90 ±03.92
	DT	77.24±10.41	75.08±15.93	77.48±14.29	91.62±04.41
	SVM	87.96±09.59	82.85±12.84	83.32±13.42	96.99±02.21
DE	KNN	79.79±17.59	78.68±17.70	81.80±15.38	85.76±12.49
	LDA	79.86±17.01	80.00±15.68	83.68±13.13	89.02±10.85
	NB	74.23±17.27	72.08± 16.51	75.97±17.01	81.38±13.56
	DT	77.43±18.09	77.22±18.13	77.82±17.53	82.63±13.58
	SVM	83.68±14.47	83.19±14.19	89.09± 07.27	91.80±07.55
WE	KNN	68.95±06.24	71.31±08.64	73.47±09.10	77.84±07.22
	LDA	72.08±06.07	74.65±06.66	75.76±07.57	79.72±06.19
	NB	70.48±06.56	75.00±07.08	75.16±09.49	77.70±07.18
	DT	64.30±07.01	65.97±08.85	71.11±10.08	74.37±08.51
	SVM	72.43±07.59	75.69±07.12	77.50±09.67	81.66±06.17
RWTE	KNN	86.86±01.01	87.61±01.00	88.93±00.87	88.48±00.91
	LDA	72.23±01.77	73.45±01.31	74.40±02.29	76.38±02.10
	NB	83.88±04.41	85.83±07.24	86.26±07.10	86.94±05.88
	DT	87.14±00.99	87.19±01.11	87.21±00.79	87.25±00.76
	SVM	90.00±00.00	90.00±00.00	91.03±00.00	92.00±00.00
PDC	KNN	89.22±02.25	88.54±02.45	89.00±02.79	89.61±02.24
	LDA	78.65±07.22	78.75±07.10	78.48±07.28	78.65±07.05
	NB	87.25±04.29	87.16±04.32	87.40±04.14	87.62±04.33
	DT	90.75±03.21	91.15±03.03	91.81±03.15	91.84±02.90
	SVM	94.72±01.55	95.24±01.23	95.31±03.19	95.51±03.59
RWTE+GTA	KNN	98.06±01.81	98.99±01.02	99.01±00.81	99.13±00.60
	LDA	98.27±01.26	98.64±01.32	97.81±01.66	98.81±00.81
	NB	92.25±04.88	92.32±05.21	93.40±02.16	93.50±03.28
	DT	98.81±00.58	98.68±00.92	99.23±00.27	99.25±00.41
	SVM	100.00±00.00	99.84±00.10	99.84±00.10	100.00±00.00
PDC+GTA	KNN	100.00±00.00	100.00±00.00	100.00±00.00	100.00±00.00
	LDA	100.00±00.00	100.00±00.00	100.00±00.00	100.00±00.00
	NB	99.69±00.22	99.62±00.35	99.64±00.20	99.64±00.13
	DT	99.25±00.93	99.64±00.16	99.61±00.10	99.22±00.31
	SVM	100.00±00.00	100.00±00.00	100.00±00.00	100.00±00.00

stimuli decreased by -10%. In line with our previous observations [64], the significant increase in the RT, suggesting a genuine reduction in the accuracy for timely responding as opposed a speed-accuracy tradeoff [65]. The increase in RT indicated that participants lose their interest in performing the task or found it stressful. The overall behavioral findings in this study is in line with previous studies that reported decline in the cognitive efficiency over time as result of mental fatigue to driving tasks [2], [40].

The functional connectivity network analysis measured by RWTE/PDC showed that, when vigilance level drops, the flow of information significantly decreased in all the frequency bands as shown in FIGURE 4 and FIGURE 5. The GTA measurements including nodal degree, clustering coefficient, global efficiency and transitivity significantly decreased with vigilance decrement indicating a loss of information exchange between brain regions as demonstrated in FIGURE 6 to FIGURE 8. Consistent with this observation,

TABLE 2. Comparisons of the average accuracies and standard deviations (%) of subject independent eeg-based semantic vigilance level classification among the various methods.

Method	Classifier	Delta	Theta	Alpha	Beta
PSD	KNN	70.33±06.78	66.54±10.54	68.44±08.44	81.58±07.55
	LDA	71.03±08.80	71.44±08.29	73.33±08.66	82.33±06.44
	NB	70.32±07.44	65.64±11.32	65.25±07.13	80.23 ±07.22
	DT	67.11±09.03	65.64±10.53	66.33±10.29	80.22±06.25
	SVM	77.64±07.08	71.25±07.27	72.22±08.52	83.22±06.33
DE	KNN	69.52±11.77	68.64±11.02	70.64±10.25	72.33±09.33
	LDA	69.44±11.22	70.33±10.33	72.44±11.03	75.22±07.25
	NB	64.28±11.33	62.24± 11.44	65.88±12.44	70.54±09.23
	DT	67.18±10.25	67.28±12.64	66.38±10.22	71.44±10.64
	SVM	71.25±09.03	72.38±10.55	77.40± 08.88	79.42±06.66
WE	KNN	60.33±05.24	61.28±03.64	63.44±6.10	66.64±05.22
	LDA	64.48±04.07	64.33±05.66	64.55±5.57	68.32±06.19
	NB	60.44±06.56	65.33±06.08	64.42±04.49	67.33±06.18
	DT	54.55±04.01	55.88±05.85	61.77±07.08	63.25±07.51
	SVM	62.88±05.59	65.52±05.12	67.44±05.67	72.23±05.17
RWTE	KNN	76.32±06.52	76.31±05.48	76.33±06.42	76.28±06.44
	LDA	64.25±05.88	65.52±05.64	66.20±04.77	67.48±04.18
	NB	72.64±06.44	75.53±08.64	76.66±08.55	77.44±05.33
	DT	76.44±05.25	77.33±04.33	77.8±04.44	78.25±05.25
	SVM	80.22±03.00	80.25±03.11	80.33±04.00	80.65±05.22
PDC	KNN	78.25±07.25	78.54±07.35	79.58±06.79	78.61±05.24
	LDA	68.64±07.33	68.33±07.25	68.48±07.23	68.55±05.05
	NB	77.13±07.03	77.16±05.25	77.40±06.33	77.26±06.33
	DT	80.25±07.03	80.15±05.03	80.64±05.22	80.64±05.90
	SVM	84.70±06.55	85.34±06.23	85.44±06.19	85.88±06.59
RWTE+GTA	KNN	86.04±03.31	86.22±01.02	86.25±03.81	86.13±03.03
	LDA	86.22±01.46	86.64±01.32	87.13±02.64	87.25±03.33
	NB	82.62±02.64	82.32±05.21	83.40±02.16	83.05±03.28
	DT	87.51±00.58	87.68±02.92	87.23±02.27	88.82±02.41
	SVM	89.02±02	89.84±02.10	90.00±01.10	90.02±02.30
PDC+GTA	KNN	89.02±02.33	89.00±02.13	89.02±02.11	90.03±03.33
	LDA	90.02±02.00	90.02±03.31	90.08±02.02	90.01±02.03
	NB	88.19±05.12	88.32±01.32	88.62±01.40	89.24±03.11
	DT	87.25±05.33	88.24±01.14	89.21±02.20	89.62±02.21
	SVM	92.12±02.11	92.64±03.03	92.88±02.00	93.08±03.13

we have previously reported a vigilance-related significant decrease of cluster coefficient and node degree over a 60-min SCWT in one frequency band at 0.1-30 Hz [64]. Previous studies have investigated various mental tasks in the single frequency bands [36], [40] and there is lack of research in essential properties in different bands.

In this paper, the functional connectivity network and graph theoretical analysis measurements were estimated in four frequency bands to measure the organization of brain functional connectivity. The statistical analysis showed significant decrement, $p<0.05$, in these analysis measurements in all the frequency bands from alert to vigilance decrement state. In particular, the highest common-decrement in the connectivity strength and topological network parameters were within the right hemisphere and over parietal-to-frontal regions demonstrated in all the frequency bands. The decrement in the connectivity network across these regions in all the frequency bands confirm the vigilance decrement. It has

been shown previously that frontal-to-parietal direction of information flux within EEG functional coupling is an intrinsic feature of brain network connectivity [66]. Our finding is in line with previous functional connectivity studies which found when mental fatigue level increases, the functional coupling decreases, specifically over the parietal-to-frontal regions in the single frequency bands [36]–[38]. The study in this paper also extended the functional connectivity and graph theoretical analysis from single band to multi-bands using two different methods of analysis. Hence, the overall decrease in functional connectivity and GTA parameters in all the frequency bands in our study is a significant indicator of vigilance decrement.

Correspondingly, in this study we found significant increase in the modularity from alertness to vigilance decrement state in all the frequency bands measured by RWTE and PDC. The increment of modularity can be interpreted as a loss of connections between the nodes due to vigilance decrement. It is worth noting that, when vigilance level drop, the information distributes and shares between modules. Thus, the overall increase in the modularity confirm the scattering of network modules or communities with decreasing vigilance level. Besides, the increment in modularity in this study was also associated with the decrement in node degree and cluster coefficient, which suggest it as a reliable index of vigilance decrement. Overall, it should be noted that the PDC and its GTA measures were much sensitive to vigilance decrement compare to RWTE. Although, the two methods are nonlinear measures reflecting the uncertainty of EEG signals, PDC is insensitive to zero-phase delay between two EEG signals occurring due to the effect of volume conduction [67].

In addition, the features extracted from RWTE/PDC alone and RWTE/PDC with their corresponding GTA measures successfully classify vigilance levels with high accuracy. RWTE features alone showed classification accuracy above 90% in subject-dependent and above 80% in the subject-independent level using SVM classifier in all the frequency bands as summarized in Table 1, and Table 2. Notably, higher accuracies of 92% and 80.65% were found in the beta frequency band for subject-dependent and subject-independent respectively. Although, other classifiers showed comparable accuracy, SVM performed better in all the frequency bands as mentioned earlier. Meanwhile, the combined RWTE and GTA features achieved 100% accuracy in the subject-dependent and above 89% accuracy in subject-independent in each of the four frequency bands using SVM classifier. The combined features of RWTE+GTA outperformed sole RWTE classification on average of +9.5% in each of the frequency bands. The higher improvement in the accuracy is due to that, GTA provide intrinsic and effective features associated with brain network characteristics. The improvement in the accuracy obtained by RWTE+GTA is also in line with previous study that utilized the directional flow of information with functional connectivity in neuro-developmental analysis and achieved 4% improvement in classification [68].

Similar improvement were also fond when combining PDC with GTA measurements indicating their complementary nature. Features from PDC alone showed classification accuracy above 94.7%, and 84.7% in subject-independent and subject-dependent level respectively in each frequency band. Meanwhile, combination of PDC+GTA features demonstrated the highest accuracy with 100% in the subject-dependent and above 92.1% in subject-independent level respectively. The combination of PDC+GTA outperformed PDC alone on average of +7%. This improvement also suggest GTA features provide complementary aspect to PDC features. It is worth noting that, the classification accuracy of PDC+GTA outperformed RWTF+GTA by +3% in all the frequency bands. This suggest PDC+GTA as a robust method for estimating vigilance levels.

Indeed, in order to highlight the important of combining strength and directionality of RWTE/PDC with their corresponding GTA parameters, we also take three baseline methods; PSD, DE and WE for comparison. The classification accuracy of all the three-baseline methods exceed 82%, 83%, and 72% in subject-dependent and 71%, 71%, and 62% in the subject independent level in all the frequency bands. Our proposed methods of PDC+GTA/RWTE+GTA significantly outperform theses baseline methods, *p<0.01* in all the frequency bands with minimum improvement of 17% in the subject dependent and 20% in the subject independent level using SVM classifier. These improvements highlight the importance of using graph theory analysis in studying the reorganization of functional connectivity in vigilance studies. We also suggest using SVM as golden standard classifier for vigilance studies. In particular, compare to other classifiers SVM yielded good performance in many applications, especially for solving problems with high dimension, nonlinearity and small dataset [69].

Although we achieved 100% classification accuracy in the subject dependent level, the maximum accuracy we achieved in the subject independent was 93.08% for beta band. This accuracy needs further improvement to establish a robust BCI system. Dimitrakopoulos et.al [40] reported 97% subject independent classification accuracy in θ band. Likewise, Wang et.al [42] utilized phase synchronization and achieved 96.76% classification accuracy using the discriminative connection features in β band. One of the reason we achieved less accuracy in the subject independent compare to [40], [42] is that we did not apply any feature selection method to select the most discriminative feature subset. Subject independent discriminative features can be obtain using sequential floating forward selection (SFFS) [70]. The kernel of SFFS can be used to iteratively select features to maximize the objective function and to remove the unnecessary contents to avoid the local maxima. Another reason may be due to the small sample size of 9-subjects in our study. Nevertheless, we should take into consideration the type of stimuli used to induce vigilance decrement. In our study we utilized SCWT which is complex and mentally demanding cognitive task compare to simple psychomotor vigilance task in [70]. The same study in [70]

achieved less accuracy of 92% when using cognitive tasks that involved mental rotation and N-back task.

Besides, our study has some limitations. First, the vigilance levels were classified into two discrete categories: alert and vigilance decrement. Vigilance could be categorized into several levels by following the recent Hourglass models of emotion in the multimodal sentiment analysis [71], [72]. Second, this study focused on vigilance classification without considering any neurofeedback. Developing an adaptive closed-loop BCI system that consists of vigilance level detection and feedback is very useful in real-time environment. In the near future, vigilance detection and prediction technologies will undoubtedly help guarantee the workplace and road safety. Third, in this study, we utilized a large number of EEG channels. Future studies should reduce the number of EEG channels by removing channels, which are relatively uncorrelated with one another across trials, or by applying a source localization method. Correlation-based channel selection [73] and weighted edit distance [74] could be potential candidates. In future work, our classification results can be further improved by utilizing deep learning, or by fusing the functional connectivity network measures with the cortical activations [49], [75]. Another area to investigate in the future to improve the classification accuracy is by combining EEG modality with functional near-infrared spectroscopy (fNIRS) [46] or Eye-tracking [76]. These modalities contain complementary information and can be integrated to construct a more robust vigilance estimation model.

VI. CONCLUSION

In the present work, we achieved semantic vigilance level classification based on a combination of RWTE/PDC and GTA measures. Experimental results revealed that RWTE+GTA and PDC+GTA perform better than sole RWTE/PDC and other baseline methods in classifying vigilance level. Besides, the highest classification accuracy was achieved using PDC+GTA with 100% accuracy in the subject-dependent and above 92.1% in subject-independent tests. The overall results indicated that the directed information flows and complex network measures provide a complementary aspect of functional connectivity and suggest PDC+GTA as very informative features for classifying semantic vigilance.
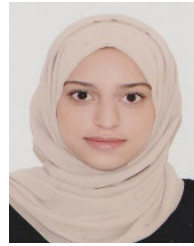
ACKNOWLEDGMENT

REFERENCES

[1] J. E. See, S. R. Howe, J. S. Warm, and W. N. Dember, "Meta-analysis of the sensitivity decrement in vigilance," *Psychol. Bull.*, vol. 117, no. 2, p. 230, 1995.

[2] F. Al-Shargie, U. Tariq, H. Mir, H. Alawar, F. Babiloni, and H. Al-Nashash, "Vigilance decrement and enhancement techniques: A review," *Brain Sci.*, vol. 9, no. 8, p. 178, Jul. 2019.

[3] J. S. Warm, R. Parasuraman, and G. Matthews, "Vigilance requires hard mental work and is stressful," *Hum. Factors, J. Hum. Factors Ergonom. Soc.*, vol. 50, no. 3, pp. 433–441, Jun. 2008.

[4] W. S. Helton and J. S. Warm, "Signal salience and the mindlessness theory of vigilance," *Acta Psychologica*, vol. 129, no. 1, pp. 18–25, Sep. 2008.

[5] J. P. Frankmann and J. A. Adams, "Theories of vigilance," *Psychol. Bull.*, vol. 59, no. 4, p. 257, 1962.

[6] A. Sahayadhas, K. Sundaraj, and M. Murugappan, "Detecting driver drowsiness based on sensors: A review," *Sensors*, vol. 12, no. 12, pp. 16937–16953, Dec. 2012.

[7] W.-L. Zheng, K. Gao, G. Li, W. Liu, C. Liu, J.-Q. Liu, G. Wang, and B.-L. Lu, "Vigilance estimation using a wearable EOG device in real driving environment," *IEEE Trans. Intell. Transp. Syst.*, vol. 21, no. 1, pp. 170–184, Jan. 2020.

[8] M. Akin, M. B. Kurt, N. Sezgin, and M. Bayram, "Estimating vigilance level by using EEG and EMG signals," *Neural Comput. Appl.*, vol. 17, no. 3, pp. 227–236, Jun. 2008.

[9] F. Li, C.-H. Lee, C.-H. Chen, and L. P. Khoo, "Hybrid data-driven vigilance model in traffic control center using eye-tracking data and context data," *Adv. Eng. Informat.*, vol. 42, Oct. 2019, Art. no. 100940.

[10] L. M. Bergasa, J. Nuevo, M. A. Sotelo, R. Barea, and M. E. Lopez, "Real-time system for monitoring driver vigilance," *IEEE Trans. Intell. Transp. Syst.*, vol. 7, no. 1, pp. 63–77, Mar. 2006.

[11] H. Yu, H. Lu, S. Wang, K. Xia, Y. Jiang, and P. Qian, "A general common spatial patterns for EEG analysis with applications to vigilance detection," *IEEE Access*, vol. 7, pp. 111102–111114, 2019.

[12] A. T. Kamzanova, A. M. Kustubayeva, and G. Matthews, "Use of EEG workload indices for diagnostic monitoring of vigilance decrement," *Hum. Factors, J. Hum. Factors Ergonom. Soc.*, vol. 56, no. 6, pp. 1136–1149, Sep. 2014.

[13] A. Martel, S. Dähne, and B. Blankertz, "EEG predictors of covert vigilant attention," *J. Neural Eng.*, vol. 11, no. 3, Jun. 2014, Art. no. 035009.

[14] S. Miquel, M. B. Haddou, and J. E. L. Day, "A systematic review and meta-analysis of the effects of mastication on sustained attention in healthy adults," *Physiol. Behav.*, vol. 202, pp. 101–115, Apr. 2019.

[15] D. R. Davies and R. Parasuraman, *The Psychology of Vigilance*. New York, NY, USA: Academic, 1982.

[16] E. Wascher, B. Rasch, J. Sänger, S. Hoffmann, D. Schneider, G. Rinkenauer, H. Heuer, and I. Gutberlet, "Frontal theta activity reflects distinct aspects of mental fatigue," *Biol. Psychol.*, vol. 96, pp. 57–65, Feb. 2014.

[17] R. Mahmoud, T. Shanableh, I. P. Bodala, N. V. Thakor, and H. Al-Nashash, "Novel classification system for classifying cognitive workload levels under vague visual stimulation," *IEEE Sensors J.*, vol. 17, no. 21, pp. 7019–7028, Nov. 2017.

[18] J. Perrier, S. Jongen, E. Vuurman, M. L. Bocca, J. G. Ramaekers, and A. Vermeeren, "Driving performance and EEG fluctuations during on-the-road driving following sleep deprivation," *Biol. Psychol.*, vol. 121, pp. 1–11, Dec. 2016.

[19] C. Zhao, M. Zhao, J. Liu, and C. Zheng, "Electroencephalogram and electrocardiograph assessment of mental fatigue in a driving simulator," *Accident Anal. Prevention*, vol. 45, pp. 83–90, Mar. 2012.

[20] C.-T. Lin, C.-H. Chuang, Y.-K. Wang, S.-F. Tsai, T.-C. Chiu, and L.-W. Ko, "Neurocognitive characteristics of the driver: A review on drowsiness, distraction, navigation, and motion sickness," *J. Neurosci. Neuroengineering*, vol. 1, no. 1, pp. 61–81, Jun. 2012.

[21] P. Parikh and E. Micheli-Tzanakou, "Detecting drowsiness while driving using wavelet transform," in *Proc. IEEE 30th Annu. Northeast Bioengineering Conf.*, Apr. 2004, pp. 79–80.

[22] J. Santamaria and K. H. Chiappa, "The EEG of drowsiness in normal adults," *J. Clin. Neurophysiol.*, vol. 4, no. 4, pp. 327–382, Oct. 1987.

[23] S. Makeig and T.-P. Jung, "Changes in alertness are a principal component of variance in the EEG spectrum," *NeuroReport-Int. J. Rapid Commun. Res. Neurosci.*, vol. 7, no. 1, pp. 213–216, Dec. 1995.

[24] J. Van Cutsem, S. Marcora, K. De Pauw, S. Bailey, R. Meeusen, and B. Roelands, "The effects of mental fatigue on physical performance: A systematic review," *Sports Med.*, vol. 47, no. 8, pp. 1569–1588, Aug. 2017.

[25] K.-Q. Shen, X.-P. Li, C.-J. Ong, S.-Y. Shao, and E. P. V. Wilder-Smith, "EEG-based mental fatigue measurement using multi-class support vector machines with confidence estimate," *Clin. Neurophysiol.*, vol. 119, no. 7, pp. 1524–1533, Jul. 2008.

[26] K. Yu, I. Prasad, H. Mir, N. Thakor, and H. Al-Nashash, "Cognitive workload modulation through degraded visual stimuli: A single-trial EEG study," *J. Neural Eng.*, vol. 12, no. 4, Aug. 2015, Art. no. 046020.

[27] F. Al-Shargie, T. B. Tang, N. Badruddin, and M. Kiguchi, "Mental stress quantification using EEG signals," in *Proc. Int. Conf. Innov. Biomed. Eng. Life Sci.* Cham, Switzerland: Springer, 2015, pp. 15–19.

[28] S. Makeig and T.-P. Jung, "Tonic, phasic, and transient EEG correlates of auditory awareness in drowsiness," *Cognit. Brain Res.*, vol. 4, no. 1, pp. 15–25, Jul. 1996.

[29] G. Borghini, G. Vecchiato, J. Toppi, L. Astolfi, A. Maglione, R. Isabella, C. Caltagirone, W. Kong, D. Wei, Z. Zhou, L. Polidori, S. Vitiello, and F. Babiloni, "Assessment of mental fatigue during car driving by using high resolution EEG activity and neurophysiologic indices," in *Proc. Annu. Int. Conf. IEEE Eng. Med. Biol. Soc.*, Aug. 2012, pp. 6442–6445.

[30] T. Paus, R. J. Zatorre, N. Hofle, Z. Caramanos, J. Gotman, M. Petrides, and A. C. Evans, "Time-related changes in neural systems underlying attention and arousal during the performance of an auditory vigilance task," *J. Cognit. Neurosci.*, vol. 9, no. 3, pp. 392–408, May 1997.

[31] A. S. Smit, P. A. T. M. Eling, M. T. Hopman, and A. M. L. Coenen, "Mental and physical effort affect vigilance differently," *Int. J. Psychophysiology*, vol. 57, no. 3, pp. 211–217, Sep. 2005.

[32] Z. Zhang, D. Luo, Y. Rasim, Y. Li, G. Meng, J. Xu, and C. Wang, "A vehicle active safety model: Vehicle speed control based on driver vigilance detection using wearable EEG and sparse representation," *Sensors*, vol. 16, no. 2, p. 242, Feb. 2016.

[33] X. Zhang, J. Li, Y. Liu, Z. Zhang, Z. Wang, D. Luo, X. Zhou, M. Zhu, W. Salman, G. Hu, and C. Wang, "Design of a fatigue detection system for high-speed trains based on driver vigilance using a wireless wearable EEG," *Sensors*, vol. 17, no. 3, p. 486, Mar. 2017.

[34] C. Papadelis, Z. Chen, C. Kourtidou-Papadeli, P. D. Bamidis, I. Chouvarda, E. Bekiaris, and N. Maglaveras, "Monitoring sleepiness with on-board electrophysiological recordings for preventing sleep-deprived traffic accidents," *Clin. Neurophysiol.*, vol. 118, no. 9, pp. 1906–1922, Sep. 2007.

[35] A. Ishii, M. Tanaka, and Y. Watanabe, "Neural mechanisms of mental fatigue," *Rev. Neurosci.*, vol. 25, no. 4, pp. 469–479, Jan. 2014.

[36] Y. Sun, J. Lim, K. Kwok, and A. Bezerianos, "Functional cortical connectivity analysis of mental fatigue unmasks hemispheric asymmetry and changes in small-world networks," *Brain Cogn.*, vol. 85, pp. 220–230, Mar. 2014.

[37] J. P. Liu, C. Zhang, and C. X. Zheng, "Estimation of the cortical functional connectivity by directed transfer function during mental fatigue," *Appl. Ergonom.*, vol. 42, no. 1, pp. 114–121, Dec. 2010.

[38] J. Chen, H. Wang, Q. Wang, and C. Hua, "Exploring the fatigue affecting electroencephalography based functional brain networks during real driving in young males," *Neuropsychologia*, vol. 129, pp. 200–211, Jun. 2019.

[39] J. Harvy, N. Thakor, A. Bezerianos, and J. Li, "Between-frequency topographical and dynamic high-order functional connectivity for driving drowsiness assessment," *IEEE Trans. Neural Syst. Rehabil. Eng.*, vol. 27, no. 3, pp. 358–367, Mar. 2019.

[40] G. N. Dimitrakopoulos, I. Kakkos, Z. Dai, H. Wang, K. Sgarbas, N. Thakor, A. Bezerianos, and Y. Sun, "Functional connectivity analysis of mental fatigue reveals different network topological alterations between driving and vigilance tasks," *IEEE Trans. Neural Syst. Rehabil. Eng.*, vol. 26, no. 4, pp. 740–749, Apr. 2018.

[41] W. Kong, Z. Zhou, B. Jiang, F. Babiloni, and G. Borghini, "Assessment of driving fatigue based on intra/inter-region phase synchronization," *Neurocomputing*, vol. 219, pp. 474–482, Jan. 2017.

[42] H. Wang, X. Liu, J. Li, T. Xu, A. Bezerianos, Y. Sun, and F. Wan, "Driving fatigue recognition with functional connectivity based on phase synchronization," *IEEE Trans. Cognit. Develop. Syst.*, early access, Apr. 13, 2020, doi: 10.1109/TCDS.2020.2985539.

[43] P. Valdez, C. Ramírez, A. García, J. Talamantes, P. Armijo, and J. Borrani, "Circadian rhythms in components of attention," *Biol. Rhythm Res.*, vol. 36, nos. 1–2, pp. 57–65, Feb. 2005.

[44] R. Brandt, D. Herrero, T. Massetti, T. B. Crocetta, R. Guarnieri, C. B. S. de Mello Monteiro, M. da Silveira Viana, G. G. Bevilacqua, L. C. de Abreu, and A. Andrade, "The Brunel mood scale rating in mental health for physically active and apparently healthy populations," *Health*, vol. 8, no. 2, p. 125, 2016.

[45] A. Delorme and S. Makeig, "EEGLAB: An open source toolbox for analysis of single-trial EEG dynamics including independent component analysis," *J. Neurosci. Methods*, vol. 134, no. 1, pp. 9–21, Mar. 2004.

[46] F. Al-Shargie, T. B. Tang, and M. Kiguchi, "Stress assessment based on decision fusion of EEG and fNIRS signals," *IEEE Access*, vol. 5, pp. 19889–19896, 2017.

[47] F. Al-Shargie, M. Kiguchi, N. Badruddin, S. C. Dass, A. F. M. Hani, and T. B. Tang, "Mental stress assessment using simultaneous measurement of EEG and fNIRS," *Biomed. Opt. Express*, vol. 7, no. 10, pp. 3882–3898, Oct. 2016.

[48] F. Al-Shargie, T. B. Tang, and M. Kiguchi, "Assessment of mental stress effects on prefrontal cortical activities using canonical correlation analysis: An fNIRS-EEG study," *Biomed. Opt. Express*, vol. 8, no. 5, pp. 2583–2598, 2017.

[49] F. Al-Shargie, U. Tariq, M. Alex, H. Mir, and H. Al-Nashash, "Emotion recognition based on fusion of local cortical activations and dynamic functional networks connectivity: An EEG study," *IEEE Access*, vol. 7, pp. 143550–143562, 2019.

[50] C. A. Frantzidis, A. B. Vivas, A. Tsolaki, M. A. Klados, M. Tsolaki, and P. D. Bamidis, "Functional disorganization of small-world brain networks in mild Alzheimer's disease and amnestic mild cognitive impairment: An EEG study using relative wavelet entropy (RWE)," *Frontiers Aging Neurosci.*, vol. 6, p. 224, Aug. 2014.

[51] Z. A. A. Alyasseri, A. T. Khader, M. A. Al-Betar, A. K. Abasi, and S. N. Makhadmeh, "EEG signals denoising using optimal wavelet transform hybridized with efficient metaheuristic methods," *IEEE Access*, vol. 8, pp. 10584–10605, 2020.

[52] Z. A. A. Alyasseri, A. T. Khader, M. A. Al-Betar, J. P. Papa, and O. A. Alomari, "EEG feature extraction for person identification using wavelet decomposition and multi-objective flower pollination algorithm," *IEEE Access*, vol. 6, pp. 76007–76024, 2018.

[53] J. Cui, L. Xu, S. L. Bressler, M. Ding, and H. Liang, "BSMART: A MATLAB/C toolbox for analysis of multichannel neural time series," *Neural Netw.*, vol. 21, no. 8, pp. 1094–1104, Oct. 2008.

[54] M. E. J. Newman and M. Girvan, "Finding and evaluating community structure in networks," *Phys. Rev. E, Stat. Phys. Plasmas Fluids Relat. Interdiscip. Top.*, vol. 69, no. 2, Feb. 2004, Art. no. 026113.

[55] M. Rubinov and O. Sporns, "Complex network measures of brain connectivity: Uses and interpretations," *NeuroImage*, vol. 52, no. 3, pp. 1059–1069, Sep. 2010.

[56] M. Rubinov, S. A. Knock, C. J. Stam, S. Micheloyannis, A. W. F. Harris, L. M. Williams, and M. Breakspear, "Small-world properties of nonlinear brain activity in schizophrenia," *Human Brain Mapping*, vol. 30, no. 2, pp. 403–416, Feb. 2009.

[57] H. W. Lilliefors, "On the Kolmogorov-Smirnov test for normality with mean and variance unknown," *J. Amer. Stat. Assoc.*, vol. 62, no. 318, pp. 399–402, Jun. 1967.

[58] H. Cai, X. Zhang, Y. Zhang, Z. Wang, and B. Hu, "A case-based reasoning model for depression based on three-electrode EEG data," *IEEE Trans. Affect. Comput.*, early access, Feb. 2, 2018, doi: 10.1109/TAFFC.2018.2801289.

[59] F. Pereira, T. Mitchell, and M. Botvinick, "Machine learning classifiers and fMRI: A tutorial overview," *NeuroImage*, vol. 45, no. 1, pp. S199–S209, Mar. 2009.

[60] F. Al-shargie, T. B. Tang, N. Badruddin, and M. Kiguchi, "Towards multilevel mental stress assessment using SVM with ECOC: An EEG approach," *Med. Biol. Eng. Comput.*, vol. 56, no. 1, pp. 125–136, Jan. 2018.

[61] I. P. Bodala, J. Li, N. V. Thakor, and H. Al-Nashash, "EEG and eye tracking demonstrate vigilance enhancement with challenge integration," *Frontiers Hum. Neurosci.*, vol. 10, p. 273, Jun. 2016.

[62] L.-C. Shi, Y.-Y. Jiao, and B.-L. Lu, "Differential entropy feature for EEG-based vigilance estimation," in *Proc. 35th Annu. Int. Conf. IEEE Eng. Med. Biol. Soc. (EMBC)*, Jul. 2013, pp. 6627–6630.

[63] A. Yildiz, M. Akin, M. Poyraz, and G. Kirbas, "Application of adaptive neuro-fuzzy inference system for vigilance level estimation by using wavelet-entropy feature extraction," *Expert Syst. Appl.*, vol. 36, no. 4, pp. 7390–7399, May 2009.

[64] F. Al-Shargie, U. Tariq, O. Hassanin, H. Mir, F. Babiloni, and H. Al-Nashash, "Brain connectivity analysis under semantic vigilance and enhanced mental states," *Brain Sci.*, vol. 9, no. 12, p. 363, Dec. 2019.

[65] C. Jacques and B. Rossion, "Early electrophysiological responses to multiple face orientations correlate with individual discrimination performance in humans," *NeuroImage*, vol. 36, no. 3, pp. 863–876, Jul. 2007.

[66] C. Babiloni, R. Ferri, G. Binetti, A. Cassarino, G. D. Forno, M. Ercolani, F. Ferreri, G. B. Frisoni, B. Lanuzza, C. Miniussi, F. Nobili, G. Rodriguez, F. Rundo, C. J. Stam, T. Musha, F. Vecchio, and P. M. Rossini, "Fronto-parietal coupling of brain rhythms in mild cognitive impairment: A multi-centric EEG study," *Brain Res. Bull.*, vol. 69, no. 1, pp. 63–73, Mar. 2006.

[67] K. J. Blinowska, "Review of the methods of determination of directed connectivity from multichannel data," *Med. Biol. Eng. Comput.*, vol. 49, no. 5, pp. 521–529, May 2011.

[68] Z. Gao, S. Li, Q. Cai, W. Dang, Y. Yang, C. Mu, and P. Hui, "Relative wavelet entropy complex network for improving EEG-based fatigue driving classification," *IEEE Trans. Instrum. Meas.*, vol. 68, no. 7, pp. 2491–2497, Jul. 2019.

[69] M. J. Abdi, S. M. Hosseini, and M. Rezghi, "A novel weighted support vector machine based on particle swarm optimization for gene selection and tumor classification," *Comput. Math. Methods Med.*, vol. 2012, pp. 1–7, Jan. 2012.

[70] P. Pudil, F. J. Ferri, J. Novovicova, and J. Kittler, "Floating search methods for feature selection with nonmonotonic criterion functions," in *Proc. 12th IAPR Int. Conf. Pattern Recognit.*, vol. 2, 1994, pp. 279–283.

[71] E. Cambria, "Affective computing and sentiment analysis," *IEEE Intell. Syst.*, vol. 31, no. 2, pp. 102–107, Mar. 2016.

[72] I. Chaturvedi, R. Satapathy, S. Cavallari, and E. Cambria, "Fuzzy commonsense reasoning for multimodal sentiment analysis," *Pattern Recognit. Lett.*, vol. 125, pp. 264–270, Jul. 2019.

[73] J. Jin, Y. Miao, I. Daly, C. Zuo, D. Hu, and A. Cichocki, "Correlation-based channel selection and regularized feature optimization for MI-based BCI," *Neural Netw.*, vol. 118, pp. 262–270, Oct. 2019.

[74] R. K. Chaurasiya, N. D. Londhe, and S. Ghosh, "A novel weighted edit distance-based spelling correction approach for improving the reliability of Devanagari script-based P300 speller system," *IEEE Access*, vol. 4, pp. 8184–8198, 2016.

[75] Z. Gao, X. Wang, Y. Yang, C. Mu, Q. Cai, W. Dang, and S. Zuo, "EEG-based spatio-temporal convolutional neural network for driver fatigue evaluation," *IEEE Trans. Neural Netw. Learn. Syst.*, vol. 30, no. 9, pp. 2755–2763, Sep. 2019.

[76] W.-L. Zheng and B.-L. Lu, "A multimodal approach to estimating vigilance using EEG and forehead EOG," *J. Neural Eng.*, vol. 14, no. 2, Apr. 2017, Art. no. 026017.

OMNIA HASSANIN (Member, IEEE) received the B.S. degree *(summa cum laude)* in electrical engineering with a minor in computer engineering from Abu Dhabi University, United Arab Emirates, in 2018. She is currently pursuing the M.S. degree in biomedical engineering with the American University of Sharjah, United Arab Emirates. She is also working as a Teacher and a Research Assistant with the Electrical Department and the Biomedical Engineering Department, respectively. Her current research interests include functional neuroimaging, signal and image processing, and machine learning.

USMAN TARIQ (Member, IEEE) received the M.S. and Ph.D. degrees from the Electrical and Computer Engineering Department, University of Illinois at Urbana–Champaign (UIUC), in 2009 and 2013, respectively. He is currently a Faculty Member with the Department of Electrical Engineering, American University of Sharjah (AUS), United Arab Emirates. Before AUS, he worked as a Research Scientist with the Computer Vision Group, Xerox Research Center Europe, France. His research interests include computer vision, image processing, and machine learning, in general while facial expression recognition and face biometrics, in particular.

HASAN AL-NASHASH (Senior Member, IEEE) is currently a Professor and an Interim Director of the Biosciences and Bioengineering Research Institute and the former Chair of the Department of Electrical Engineering, American University of Sharjah. He designed and developed several electronic instruments to measure various biodynamic parameters. He is leading the effort to establish the Biosciences and Bioengineering Research Institute, AUS, and has previously led the effort to establish the M.S. graduate program in biomedical engineering. He is the author of more than 100 journal and conference papers, five book chapters, and two issued U.S. patents. His research interests include neuroengineering, signal processing, and microelectronics. He played an active role in organizing several biomedical and electrical engineering conferences. He is the former Middle East and Africa Representative on the IEEE-EMBS Administrative Committee. He worked closely with several biomedical engineering departments and hospitals, including the National University of Singapore, Johns Hopkins University, and Rashid Hospital, Dubai.

FARES AL-SHARGIE (Member, IEEE) received the B.S. and M.S. degrees in biomedical engineering from Multimedia University, Malaysia, and the Ph.D. degree in biomedical engineering from Universiti Teknologi PETRONAS, Malaysia. He is the first author in more than 30 journal and conference papers, one book, and one book chapter. He worked closely with several biomedical engineering departments and companies, including Hitachi Ltd., Research and Development Group, Japan. His current research interests include the assessment of mental stress, vigilance decrement, and emotions via, EEG, fNIRS neuroimaging modalities, and eye tracking. He is a member of the Society of Functional Near-Infrared Spectroscopy.

• • •